Studies on the Biodegradation and Biocompatibility of a New Poly(ester amide) Derived from L-Alanine

N. PAREDES,[1] A. RODRIGUEZ-GALÁN,[1] J. PUIGGALÍ,[1] C. PERAIRE[2]

[1] Departament d'Enginyeria Química, ETS d'Enginyers Industrials, Universitat Politècnica de Catalunya, Diagonal 647, Barcelona 08028, Spain

[2] Centro de Investigación y Desarrollo Aplicado, s.a.l., Argenters 6, Sta Perpetua de Mogoda 08130, Spain

Received 23 June 1997; accepted 15 January 1998

ABSTRACT: A new poly(ester amide) derived from L-alanine has been synthesized and characterized. The polymer has good fiber- and film-forming properties, as well as other characteristics like thermal stability and solubility in chloroform, which enhance its processing facilities. Degradation studies show that both pH and temperature influence in the hydrolisis rate that takes mainly place through the ester linkages. Degradation was also studied by using different enzymes. Results indicated that papain was the most efficient of these, and that the hydrolysis to water-soluble products could be attained in a few days. Basal cytotoxicity was assayed using a mouse L929 fibroblast permanent cell line. The MTT viability test was performed with liquid extract of the material (50 days, 37°C). An attachment and proliferation screening study with intact material was also carried out. No cytotoxic responses were detected, in either assay, after a 24- and 48-h incubation period with the cells. After 72 h a slight cytotoxicity was detected in the polymer material, while a more significant one was detected in the material extract. © 1998 John Wiley & Sons, Inc. J Appl Polym Sci 69: 1537–1549, 1998

Key words: biocompatibility; enzymatic degradation; hydrolytic degradation; poly(ester amide); L-alanine

INTRODUCTION

The biodegradation of synthetic polymers is a subject of considerable interest for environmentalists and industrialists. A considerable effort has also been made to obtain polymers with appropriate properties for biomedical applications such as bioabsorbible sutures, bone fixation, and implants. Although several series of aliphatic polyesters (mainly derived from lactic[1] and/or glycolic[2] acids) are commercially available for these purposes, they still lack certain optimum properties such as mechanical, thermal, and processing[3] properties. Different nylons have also been investigated because the hydrogen bond interactions between neighboring chains may improve some of these properties. However, their rate of degradation proves too small for them to be considered as commercial biodegradable polymers. Inclusion of α-amino acids favors the susceptibility to enzymatic degradation. Thus, different poly(α-amino acids)[4] and nylons containing α-amino acids (i.e., copolymers of 6-aminohexanoic acid and glycine,[5,6] and 11-aminoundecanoic acid and L-alanine[7]) have been tested. In general, these materials are difficult to process, especially when the amide/methylene ratio is high. Aliphatic poly(ester amide)s have been suggested and recently in-

Correspondence to: J. Puiggalí.

Contract grant sponsor: CICYT; contract grant number: MAT -97–1013.

Contract grant sponsor: Comissió Interdepartamental de Recerca i Innovació Technològica.

Journal of Applied Polymer Science, Vol. 69, 1537–1549 (1998)

 CCC 0021-8995/98/081537-13

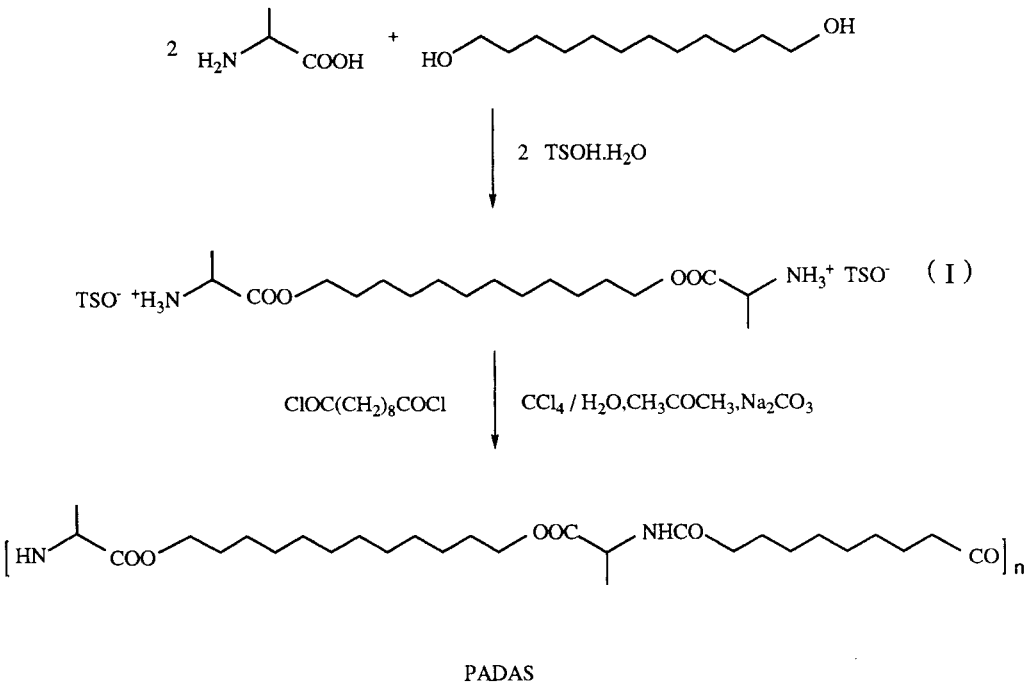

Abbreviations:
TSOH: p-toluenesulfonic acid

PADAS: Polyesteramide derived from L-alanine (A), 1,12-dodecanediol (D) and sebacic acid (S).

Scheme 1

vestigated[8] as a potential family of polymers with optimum behavior: mechanical and thermal due to the amide groups and degradability due to the ester groups. In this work we study a poly(ester amide) derived from an α-amino acid like L-alanine and, therefore, with a potentially enhanced biodegradability. The synthesis of related polymers from α-amino acid glycol esters and dicarboxylic acids has been previously reported.[9]

EXPERIMENTAL

All chemicals were ACS grade and used without further purification. The polymer (PADAS) was synthesized from the α-amino acid glycol ester according to the two-step methodology previously reported for other derivatives and outlined in Scheme I.

Monomer Synthesis

A three-necked round-bottom flask equipped with a $CaSO_4$ drying tube, magnetic stirrer, and a Dean-Stark apparatus was charged with L-alanine (0.272 mol), *p*-toluene–sulfonic acid monohydrate (0.272 mol), dodecanediol (0.123 mol), and toluene (750 mL). Then, the reaction medium was refluxed until no more water was distilled out (10 h). The mixture was cooled at room temperature and then a viscous oil separated from the toluene solution. After drying at vacuum, the recovered hard solid was recrystallized twice from isopropanol to give 64 g (75%) of a white solid; m.p. 168–169°C.

IR (KBr) 2922 and 2850 (CH_2), 1738 (C=O); ^{1}H-NMR ($CDCl_3$/TFA) δ 7.7–7.2 (8H, m, Ar-H), 4.30 (2H, m, CH), 4.21 (4H, m, $COOCH_2$), 2.41 (6H, m, Ar-CH_3), 1.72 (6H, d, CHCH_3), 1.65 (4H, m, $COOCH_2CH_2$), 1.30, (16H, m, $COOCH_2CH_2$-(CH_2)$_8$).

ANAL. Calcd. for $C_{32}H_{52}N_2O_{10}S_2$: C, 55.73; H, 7.55; N, 4.06. Found: C, 55.80; H, 7.46; N, 4.02.

Polymerization

The poly(ester amide) was synthesized by interfacial polymerization of the monomer (I) and sebacoyl dichloride. The method was adapted from the general procedure used for the synthesis of nylons[10] that has been employed by Huang for poly(esteramides).[9]

A solution of the monomer (0.033 mol) and the proton acceptor (0.066 mol of Na_2CO_3) in a mixture of water (340 mL) and acetone (22 mL) was added to 225 mL of a solution of the dichloride (0.033 mol) in CCl_4. Although a brittle film immediately appeared in the interphase, the polymerization was optimized when the reaction mixture was stirred at high speed in a reactor vessel. After 30 min, the polymer was filtered and repeatedly washed with CCl_4, water, ethanol, and ether before drying in a vacuum desiccator at 60°C.

Molecular Weight Determination

The intrinsic viscosity of the samples was determined by measurement with a Cannon-Ubbelhode microviscometer in dichloroacetic acid solutions at 25 ± 0.1°C. The molecular weight distributions (M_n, M_w, and polydispersity index) were measured with a GPC apparatus (Water Assoc., Model 510) equipped with a Maxima 820 computer program. M_n and M_w values are indicative because they were calculated using polystyrene standards (Polysciences). A set of two μ-Styragel (Polymer Lab.) columns with limited exclusion molecular weight of 10^4 and $10,^3$ and a RI 410 (Water Assoc.) detector were used. The polymer was dissolved and eluted in chloroform at the flow rate of 0.5 mL/min (injected volume 100 μL, sample concentration 0.35% w/v).

Spectroscopy

Infrared absorption spectra were recorded from potassium bromide pellets with a Perkin-Elmer 1600 FTIR spectrometer in the 4000–500 cm^{-1} range. NMR spectra were registered from polymer solutions in deuterated chloroform using tetramethylsilane (TMS) as an internal standard. A Bruker AMX-300 spectrometer operating at 300.1 and 75.5 MHz was used for ^1H- and ^{13}C-NMR investigations, respectively. A sine bell window function was employed in the Fourier transform of 2d NMR data matrices to suppress peak broadening.

Thermal Analysis

The thermal behavior was studied by differential scanning calorimetry with a Perkin-Elmer DSC-4 and a Mettler DSC-30 to determine the melting (T_m) and glass transition (T_g) temperatures of the samples. Indium metal was used for calibration purposes (T_m = 429.75 K, ΔH_f = 3.267 kJ/mol). Thermogravimetric analysis was carried out with a Mettler TG50 thermobalance. Unless otherwise noted, heating and cooling rates were 10°C/min. All experiments were done under a flow of dry N_2, through the calorimeter.

X-ray Diffraction

Powder X-ray diagrams were recorded under vacuum conditions at room temperature and calcite (d_B = 3.035 A) was used for calibration. A modified Statton camera (W. H. Warhus, Wilmington, DE) with a nickel-filtered copper radiation of wavelength 1.542 A was used for these experiments.

Degradation Studies

Samples for hydrolytic and enzymatic degradation studies were prepared by melt pressing at ca. 110°C (10°C below the melting temperature of the polymer). Discs with a diameter of 12 mm were prepared and those with a thickness of 200–300 μm and a weight of 30–45 mg were selected. For the hydrolysis experiments each disc was kept in bottles filled to 30 mL with one of the following buffers: (a) 0.1 aqueous Na_2HPO_4/KH_2PO_4 (pH 7.4); (b) 0.1*M* aqueous citrate/HCl (pH 2.3); (c) 0.1*M* aqueous $Na_2CO_3/NaHCO_3$ (pH 10.6). Sodium azide (0.03 wt %) was used to prevent microbial growth. Two temperatures were selected for hydrolysis so the vials were kept in ovens maintained at 37 and 70°C. After the immersion time, the retrieved samples were thoroughly rinsed with water, dried to constant weight in vacuum, and stored over $CaCl_2$ before analysis.

The enzymatic degradation with papain was carried out in a 0.05*M* phosphate buffer (pH 6.0). Papain (30 000 USP-U mg^{-1} No. 7144) was purchased from Merck, and was used without further recrystallization. The proteolytic enzyme was activated in the buffered solution with 34 m*M* L-

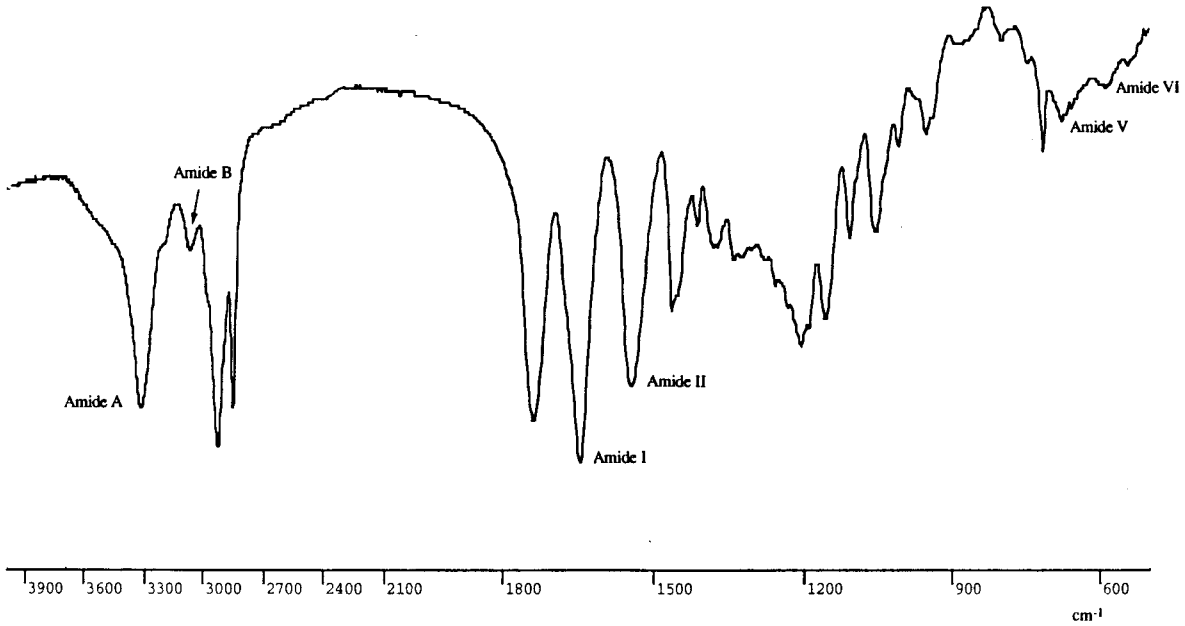

Figure 1 Infrared spectra of PADAS. Note the relative sharp band corresponding to the Amide I mode, which is indicative of a unique type of hydrogen bonds.

cysteine and 30 m*M* ethylenediaminetetraacetic disodium salt in a procedure similar to that proposed by Arnon.[11] Sodium azide (0.03 wt %) was also used. The stability of the enzyme under experimental conditions was controlled by the use of a high molecular-weight substrate such as casein. The activity of the papain was determined by measuring the absorbancy of the solution at 280 nm. Polymer samples were placed in small bottles containing 10 mL of the enzymatic medium. The reaction solution was incubated at 37°C from 1 to 360 h and the enzyme solution was renewed after every 72 h because of the enzymatic activity loss (around 15%). After incubation, the retrieved samples were washed and dried as indicated before for the hydrolytic experiments. In all cases, the mass loss and the intrinsic viscosity of the samples were evaluated.

Degradation in a cell culture media was carried out by using minimum essential medium (MEM) with Earle's salts (Sigma 0268). Films were prepared by slow evaporation of polymer solutions in $CHCl_3$ (10% w/v) and cut into discs similar in diameter, weight, and thickness to those used for hydrolitic degradation. The discs were placed in a tissue culture multiwell plate, where each well was filled to 1.5 mL with the culture medium. After incubation at 37°C, the samples were treated as previously indicated.

Biocompatibility

For the citotoxicity studies, a film of the polymer was prepared by the slow evaporation at 37°C, of a dilute chloroform solution (10% w/v) onto Petri dishes. Subsequently, the film was cut into discs with a diameter of 6 mm (surface (S): 0.28 cm^2) for the evaluation of polymer basal citotoxicity and into a film of 12 cm^2 for the evaluation of the citotoxicity of the degradation products. The samples were sterilized by gamma irradiation using a dose of 25 kGy. The permanent cell line used was L929 mouse fibroblast (ATCC, CCL1, NCTC 929) cultured in MEM, 10% Foetal Calf Serum (JRH Bioscience), 1% Penicillin–Streptomycin, and 1% Glutamine.

The basal cytotoxicity of the polymer was determined by using standard methods.[12,13] To detect the cytotoxicity of the intact material, 1×10^4 L929 mouse fibroblasts were seeded onto each material and negative control samples. We used tissue-culture grade polystirene plastic (NUNC) as a negative control and a phenol solution of 0.64 mg/mL as positive cytotoxic control. The cultures were incubated for 24, 48, and 72 h at 37°C and 5.5% of CO_2. After that, the cellular counts were carried out with a micrometric eye piece. The kinetic growth and doubling time were calculated. The level of cytotoxicity for each parameter was calculated as a percentage of the corresponding

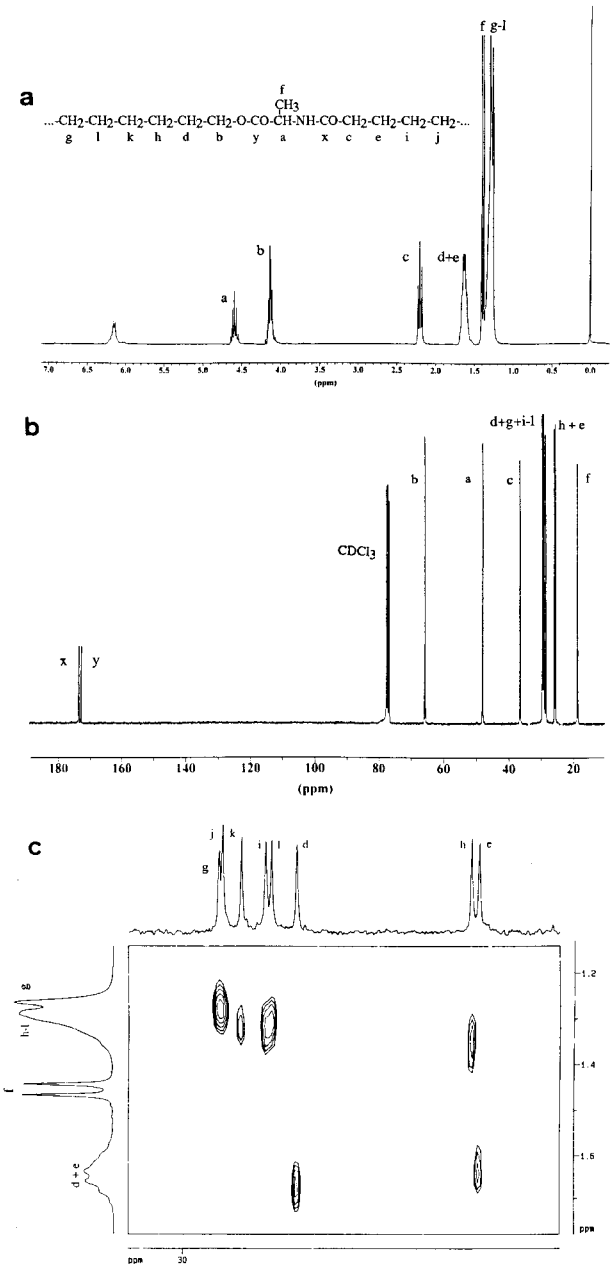

Figure 2 ^{1}H (a), ^{13}C (b) and two-dimensional (c) NMR spectra of PADAS. Assignment of peaks is carried out according to the inset scheme that represents half of the symmetric repeat unit.

values for the negative control group (a substance is considered cytotoxic if this percentage is greater than 25%).

The cytotoxicity of the products released was evaluated with a cell metabolic test. The material was previously incubated in MEM for 50 days at 37°C and an initial PH of 7.2, in a borosilicate glass container (with a surface/volume ratio of 3 cm^2/mL) without agitation. Other containers with the same extraction vehicle but without the test material were prepared under the same conditions to provide controls for the testing procedure. At the end of the incubation period, the material extract and controls were put in contact with semiconfluent cultures in 96-well plates, at selected concentrations (100, 50, 25, and 10%). A phenol solution at concentration of 6.4 mg/mL was used as a positive control. Three cultures were evaluated for each time point, concentration, and material tested (screening study). After 24 and 72 h of incubation at 37°C and 5.5% of CO_2, the metabolic activity test (MTT, water-soluble tetrazolium dye, 3-(4,5-dimethylthiazol-2-yl)-2,5-diphenyl-2*H*-tetrazolium bromide) was performed. The optical density was measured at 540 nm.

RESULTS AND DISCUSSION

Synthesis and Characterization

The polymer was obtained with a high yield and purity from interfacial polymerization. Thus, a yield of around 80–90% was found in all the polymerizations carried out, being the best elemental analysis: C, 65.63; H, 9.73; N, 5.07. Calcd for $C_{28}H_{50}N_2O_6$: C, 65.88; H, 9.80; N, 5.49. A limited intrinsic viscosity of ca. 0.60 dL/g was found although different reaction conditions were tested to increase the degree of polymerization. Thus, the proportion of acetone used to solubilize the L-alanyl monomer (I) in the aqueous phase was optimized as well as other factors like the types of proton acceptor and organic solvent.

Average molecular weights of 9000 and 24,100 for M_n and M_w (polydispersity index of 2.67) could be deduced from the GPC analysis. However, the molecular weight was sufficient to give film- and fiber-forming properties. PADAS shows good solubility in strong acids as is usual in polyamides (formic, dichloroacetic, and trifluoroacetic acid) and polar organic solvents like dimethylsulfoxide, dichloromethane, and chloroform, which enhance the processing facilities from solution. The infrared spectrum (Fig. 1) of the PADAS polymer shows the characteristic absorptions bands corresponding to the amide (3316, 3072, 1650, 1540, 684, and 584 cm^{-1}), methylene (2924, 2844, and 722 cm^{-1}), and ester (1740, 1160, and 1060 cm^{-1}) groups. It should be noted that the appearance (single peaks with no shoulders) and the position of the amide bands indicate a strong and unique

Table I Assignment of the ^{1}H- and ^{13}C-NMR Spectra from Deuterated Chloroform Solutions of PADAS (δ, ppm)

	g	l	k	h	d	b	y	a	f		x	c	e	i	j
	~~CH_2—CH_2—CH_2—CH_2—CH_2—CH_2—OOC—CH								(CH_3)—NH—CO—CH_2—CH_2—CH_2—CH_2~~						
^{1}H	1.30	1.30	1.30	1.30	1.63	4.13		4.59	1.39	6.14		2.20	1.63	1.30	1.30
^{13}C	30.30	29.51	29.96	25.79	29.13	65.62	172.6	47.96	18.70		173.4	36.51	25.52	29.60	30.25

kind of hydrogen bonds. Thus, no evidence of amide–ester hydrogen bonds has been detected, although their coexistence with the amide–amide hydrogen bonds has been reported in some cases.[14] Moreover, these absorptions and specifically those corresponding to the high conformationally sensitive region of 700–500 cm^{-1} appear very close to the characteristic values of nylons in their extended conformation[15] (i.e., 690 and 580 cm^{-1} for the Amide V and VI bands of nylon 6 in its α-form, respectively). Note also that the position of the Amide I is closer to the expected value for nylons in their extended conformation than is expected for poly(α-amino acid)s in their β-sheet structure[16] (1645 vs. 1630 cm^{-1}).

NMR spectra (^{1}H and ^{13}C) are fully consistent with the anticipated polymer constitution [Fig. 2(a) and 2(b)]. Two-dimensional NMR was also recorded to ensure a rigorous and detailed assignment (Table I) in terms of coupling/decoupling among the nuclei as shown in Figure 2(c). In agreement with the molecular weight measurements we could not detect any peak corresponding to terminal groups in both NMR spectra.

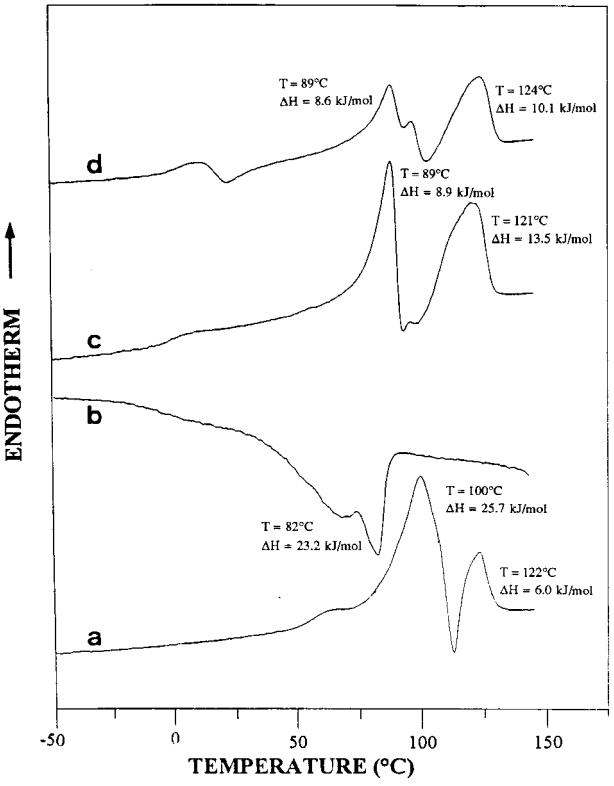

Figure 3 Sequence of four DSC traces for a PADAS sample recovered directly from the synthesis medium: run a, heating of the original sample; run b, cooling; run c, reheating; run d, reheating after fast cooling. Rate in all cases was 10°C/min.

Thermal Behavior

All fusion data (temperatures and heats of fusion) are included in Figure 3 for the four runs performed with the polymer sample coming directly from polycondensation. In the first run [Fig. 3(a)] the sample was heated at 10°C/min through fusion and left in the melt for 2–3 min. Subsequent cooling was performed at the same speed to observe crystallization from the melt [Fig. 3(b)]. A second heating was performed to check the reproducibility of the transitions and get data for the melt-crystallized sample [Fig. 3(c)]. Figure 3(d) corresponds to the heating run of a melt-quenched sample to the lowest temperature that can be achieved, −100°C, to observe glass transition and determine whether crystallization could be suppressed. This calorimetric analysis indicates thermal stability because there are well-behaved melt baselines after fusion and the transitions observed on heating are reproducible. In general, the thermograms contain well-defined peaks corresponding to both melting and crystallization transitions. Double melting peaks are seen in all the heating runs, a very common observation in thermal studies of polyamides.[17] These studies indicate that the double-peak effect is the result of a recrystallization process affecting the population of smaller crystals with a lower melting point. To corroborate this assertion for the PADAS poly-

(ester amide) we registered the DSC thermograms at different heating rates (Fig. 4). It can be seen that the DSC scans registered at increasing heating rates show a significant increase in the heat of fusion associated with the low-temperature endotherm, while the total amount of energy absorbed by the sample remains approximately constant. Such evolution is the familiar pattern associated with "reorganization" during heating. Note that, at the low heating rates (lower than 20°C/min) a small exotherm indicative of cold crystallization precedes the higher melting peak, the latter being entirely suppressed when the heating rate is 80°C/min. These cold crystallization peaks can also be clearly observed in the melt-crystallized and melt-quenched samples at a heating rate of 10°C/min [Fig. 3(c) and (d)]. On the other hand, X-ray diffraction data from different samples, as described below, permit us

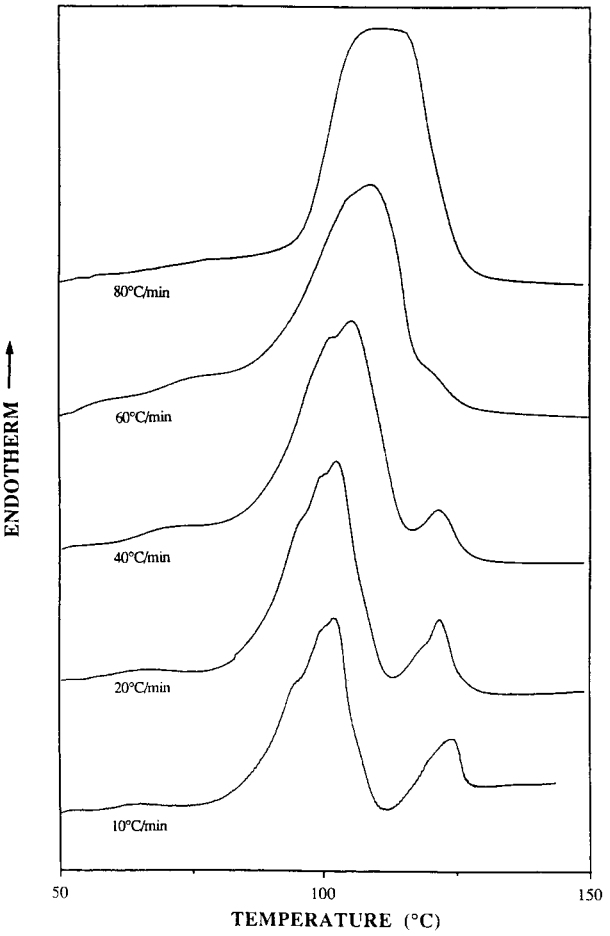

Figure 4 Thermograms of PADAS obtained with scanning rates ranging from 10°C/min to 80°C/min. Note that the cold crystallization and the high melting peaks disappear when the scanning rate increases.

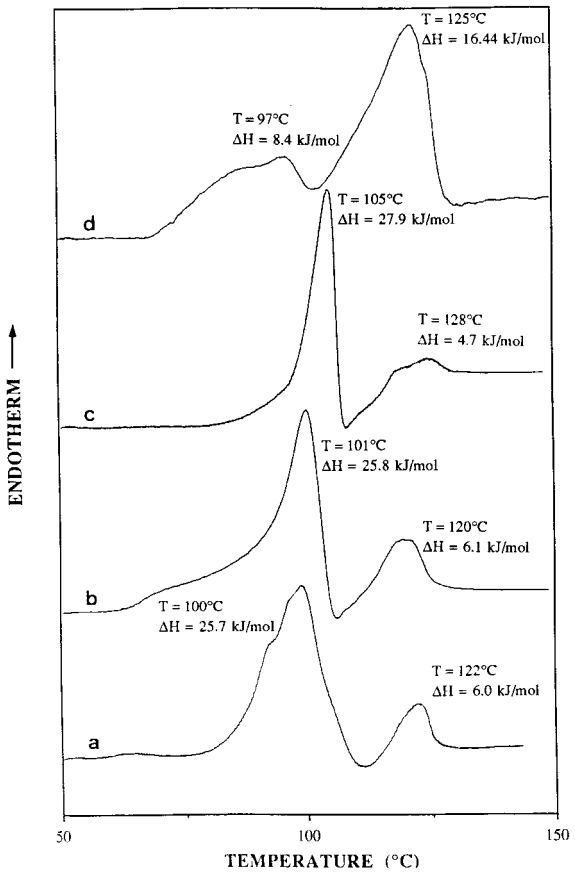

Figure 5 DSC traces of different samples of PADAS: (a) polymer coming directly from polycondensation; (b) film prepared by slow evaporation from a chloroform solution; (c) polymer crystallized in a butanediol solution at 50°C; (d) film prepared by melt pressing. The heating rate in all cases was 10°C/min.

to discard a polymorphic transition. A glass transition temperature of 0.7°C can be deduced from Figure 3(d) where an additional cold crystallization peak at 22°C can be observed. This glass transition temperature is intermediate between those temperatures expected for similar polyesters and polyamides.[18] However, a baseline change at 56.4°C and very close to the characteristic T_g of related polyamides is clearly observed in Figure 3(a). This fact may suggest that segments constituted by amide groups are predominant in the amorphous material of samples recovered from polycondensation. Sample preparation greatly affects the crystallinity and the distribution of the populations of crystals. Figure 5 compares the first heating run of different samples: (a) PADAS sample obtained directly from polycondensation, (b) film prepared by slow evaporation of a chloroform solution, of the type that will be used in the

Table II Experimental Heats of Fusion and Estimated Crystallinities for Different PADAS Samples

Sample	ΔH_1 (kJ/mol)[a]	ΔH_2 (kJ/mol)[a]	% W_c[b]
Recovered from polymerization	25.7	6.0	35.8
Melt crystallized	8.9	13.5	25.3
Quenched from the melt	8.6	10.1	21.1
Film from chloroform	25.8	6.1	36.0
Crystallized from butanediol at 50°C	27.9	5.7	36.8
Melt pressed	8.4	16.4	28.1

[a] The heats of fusion ΔH_1 and ΔH_2 correspond to the first and second melting peaks, respectively.

[b] Crystallinity evaluated supposing a ΔH_f^{eq} of 88.4 kJ/mol according to the group contributions[19] to the heat of fusion.

citotoxicity essays, (c) polymer crystallized in a diluted 1,4-butanediol solution at 50°C, and (d) melt-pressed film, of the type used for degradation studies.

The crystallinity of samples could be evaluated by using the heat of fusion for a 100% crystalline material (ΔH_f^{eq}), which was estimated from the reported[19] group contributions of ester (−2.5 kJ/mol), amide (2.0 kJ/mol), CH(CH_3) (4.7 kJ/mol), and methylene (4.0 kJ/mol). Thus crystallinities around 37% are characteristic of solution crystallized samples, whereas the recovery of crystallinity on melt-crystallized or quenched samples is about 60% [Figs. 3(c), (d), and 5(d)]. Note also (Table II) that, in these samples, the proportion of the high melting peak increases, suggesting a preferential crystallization from the melt in the high temperature state. Figure 6 shows the characteristic X-ray diffraction pattern of the different PADAS samples. In general, the patterns are similar, whichever the melting peak predominating in the sample. This fact gives support to the supposition that the double melting peak does not correspond to a polymorphic transition.

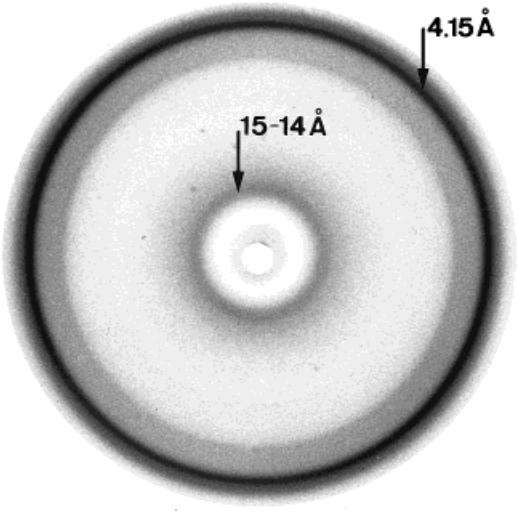

Figure 6 Characteristic X-ray powder pattern of a PADAS sample. In this case the sample was prepared by thermal annealing at 110°C and its thermogram is similar to that depicted in Figure 5(d). Note the high intensity of the 4.15 Å reflection, which is associated to the chain packing as usual in polyamides and polyesters. On the contrary, the low angle reflection (15–14 Å), which is associated to the chain repeat, appears broad and diffuse.

Thermogravimetric analysis shows that PADAS is stable through fusion and so the applicability of the polymer is not impaired. The $T_{d,0}$ decomposition temperature (inclination point in the loss of weight vs. temperature curve) appears at 210°C (more than 80°C after fusion). Fifty percent of weight loss occurs at 330°C in a decomposition process that takes place in two steps. Furthermore, no changes after fusion have been detected in the ^{13}C-NMR spectra of samples maintained for 10 min at 140°C. This fact indicates that reactions of transamidation-transesterification do not occur during the melting process.

Hydrolytic Degradation

The hydrolytic degradation of PADAS was carried out at 37°C in buffers of pHs 7.4, 10.6, and 2.3. To verify the influence of the temperature on the hydrolysis an assay at pH 7.4 was also realized at 70°C. Weight loss measurements, GPC analysis and viscosity determinations (Tables III and IV) showed that PADAS is degradable, as indicated by the decreases of the corresponding parameters.

Table III Erosion, Viscosity, and Molecular Weight Changes during the Hydrolytic Degradation of PADAS at 37°C

	pH = 2.3			pH = 7.4			pH = 10.6		
Degrad. Days	% Weight Remaining	$[\eta]$[a] (g/dL)	M_w[b]	% Weight Remaining	$[\eta]$[a] (g/dL)	M_w[b]	% Weight Remaining	$[\eta]$[a] (g/dL)	M_w[b]
0	100.0	0.58	24,100	100.0	0.58	24,100	100	0.58	24,100
2	99.8	0.57	—	—	—	—	100	0.54	23,900
5	99.7	0.54	—	99.5	0.55	23,100	99.5	0.43	—
7	98.6	0.53	22,100	—	—	—	99.5	0.39	22,100
22	99.6	0.48	19,800	97.8	0.48	20,500	99.5	—	21,200
51	98.9	0.41	18,400	98.4	0.44	18,600	98.1	0.33	16,500
75	—	—	—	97.9	0.41	17,200	96.6	0.30	14,900
111	98.7	0.24	16,000	98.8	0.38	—	—	—	—
195	—	—	—	97.6	0.30	12,000	—	—	—
305	—	—	—	94.5	0.25	9,100	—	—	—

[a] Intrinsic viscosity measured in dichloroacetic acid at 25°C.
[b] Molecular weight determined by GPC.

The evolution of the M_w of PADAS during incubation is represented in Figure 7(a), which shows that the relative order of PADAS hydrolytic degradation is as follows: 70°C, pH 7.4 > 37°C, pH 10.6 > 37°C, pH 2.3–37°C, pH 7.4. Observation of this figure clearly demonstrates that PADAS degrades at 37°C in a slow but steady way. The tendency to degradation of PADAS at pH 2.3 and pH 7.4 is nearly identical, but it increases slightly in the basic buffer at pH 10.6

On the other hand, the influence of temperature on the degradation of PADAS is significant as can be corroborated in Table IV and Figure 7(a). At 70°C and pH 7.4, the molecular weight of PADAS decreases to one-half of its initial value in 6 days, whereas the same change in the buffer at 37°C and pH 7.4 took place during an interval of 195 days.

Table IV Data of the Hydrolytic Degradation of PADAS at 70°C

	pH = 7.4		
Degrad. Days	% Wt Remaining	$[\eta]$[a] (g/dL)	M_w[b]
0	100.0	0.58	24,100
6	98.1	0.48	12,900
16	94.5	0.35	9,800
52	85.9	0.27	7,100
65	83.7	0.24	6,500
100	77.1	0.16	6,000

[a] Intrinsic viscosity measured in dichloroacetic acid at 25°C.
[b] Molecular weight determined by GPC.

Figure 7(b) shows the % weight remaining of PADAS after hydrolytic degradation in the four conditions mentioned above. In general, at 37°C the observed weight losses are minimal. Thus, whatever the pH of the buffers used in the experiments, the weight losses after 75 days of hydrolysis are less than 3.5%. They are similar at pH 2.3 and 7.4, whereas a slightly superior value is observed at pH 10.6. When the experiment at 37°C and pH 7.4 was continued for 305 days, a final weight loss of 5.5% was obtained. In contrast, when PADAS was degraded at 70°C and pH 7.4, the weight loss measured after 100 days of incubation was 22.9%.

The small changes observed in the weight of the discs during the incubation of PADAS at 37°C, could be explained in two ways. On the one hand, the change in the size of the molecules is not considerable, as can be verified if the number of chain bonds split per molecular chain (estimated as $N = M_{n_{(o)}}/M_{n_{(t)}} - 1$) is calculated for the experiment realized at pH 7.4. As the initial M_n is 9000 and the final M_n (after 305 days) is 5100, only 0.764 bonds per molecule are split. On the other hand, PADAS has been prepared from monomers with a high content in hydrophobic methylene groups. Based on these considerations, it must be expected that the oligomers produced in the degradation of PADAS are not readily soluble in the aqueous medium at 37°C.

When the degradation is carried out at 70°C,

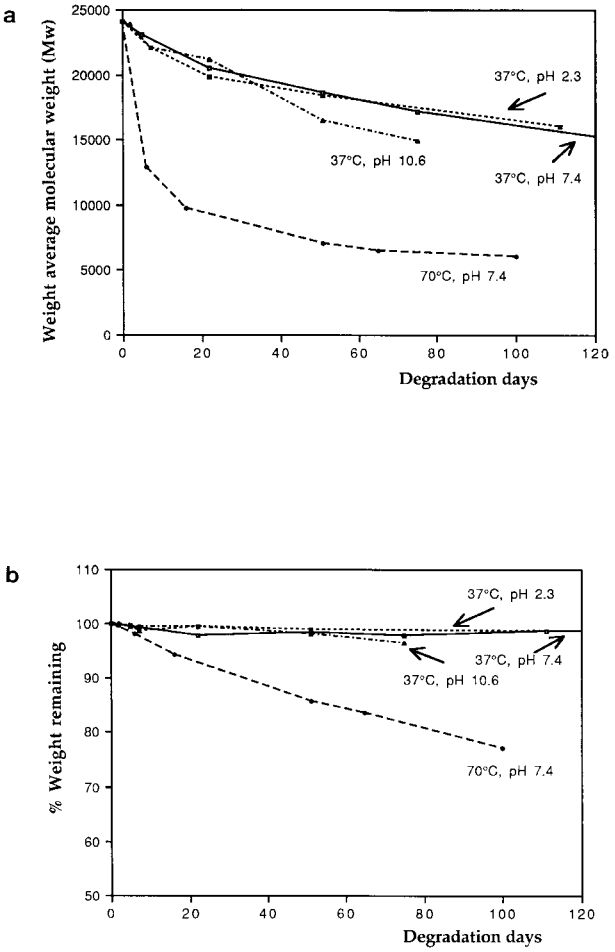

Figure 7 (a) Plot of M_w vs. degradation time (days) for discs of PADAS during hydrolytic degradation in the conditions indicated. (b) Changes in the remaining molecular weight of discs of PADAS after hydrolytic degradation in the conditions indicated.

the weight loss is much greater than that measured at 37°C. This is probably due to the larger extension of the degradation yielding smaller oligomers, and also to the greater solubility of the produced oligomers in an aqueous medium heated to 70°C.

The ^{1}H-NMR spectra of three samples of PADAS after 22, 111, and 305 days of hydrolytic degradation at 37°C and pH 7.4 are compared in Figure 8. Of primary importance to a discussion of the results of NMR analysis is that, with degradation time, there is both an increase in the area of the peak at 3.65 ppm and a decrease in the area of the peak at 4.16 ppm.

The first peak corresponds to the α-methylene of unesterified 1,12-dodecanediol, whereas the second one is assigned to the analogous methylene

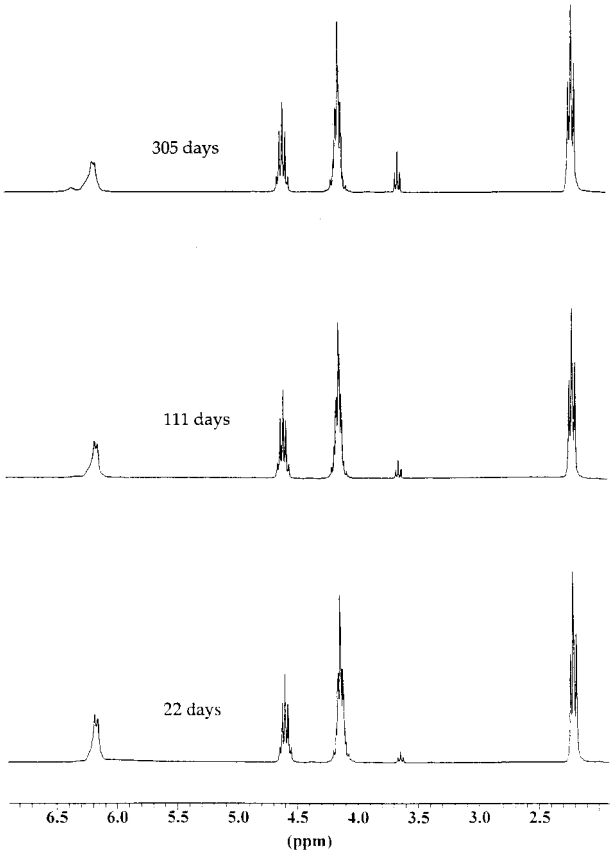

Figure 8 ^{1}H-NMR spectra of PADAS after 22, 111, and 305 days of hydrolytic degradation in a pH 7.4 phosphate buffer at 37°C.

of a 1,12-dodecanediol esterified unit. Therefore, the NMR analysis seems to indicate that, during degradation, there is a hydrolysis of the ester groups formed by the —OH of diol and the —COOH groups of L-alanine.

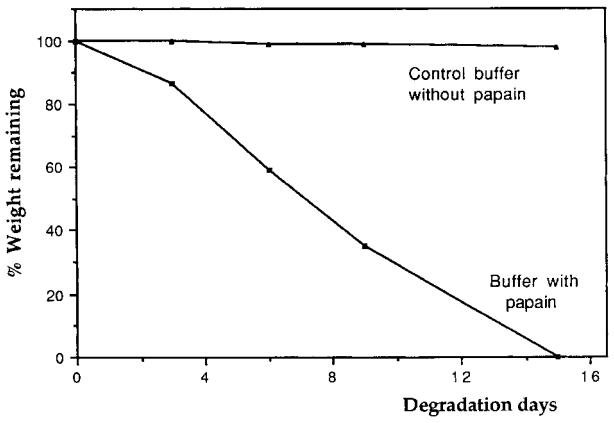

Figure 9 Percentage of weight remaining of PADAS during enzymatic degradation in a buffer with papain.

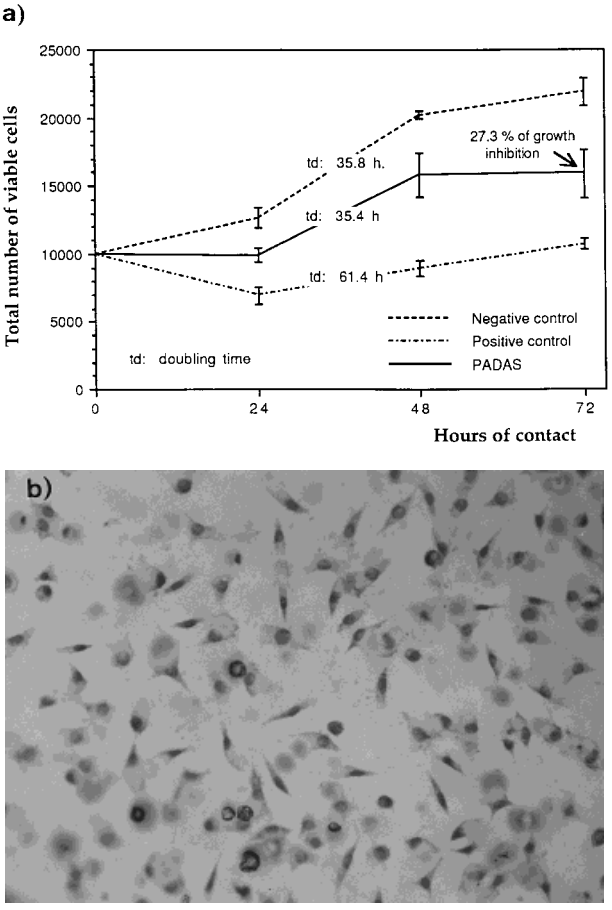

Figure 10 Proliferation of a culture of L929 fibroblasts on PADAS surface: (a) proliferation curve, (b) semiconfluent culture after 48 h (Giemsa, 100.8×).

Moreover, the peak assigned to the α-methylene of esterified sebacic acid (2.20 ppm) does not change during the incubation time, revealing that there is no hydrolysis of amide groups during degradation. That is, the degradation of the polyesteramide PADAS takes place preferentially in the ester bonds of the main chain and so the amide groups remain unchanged.

Because a part of the cytotoxic studies was developed after incubation of PADAS in a minimum essential medium (MEM), its hydrolytic degradation was also monitored in this system for 50 days. Results indicate that, in this period of time, PADAS loses a 5% of its initial weight, whereas M_w and M_n decrease to 18,700 and 7200, respectively.

These data demonstrate that PADAS also degrades in this solution, and that the biological behavior of an extract of PADAS in MEM must be attributed to the 5% of material that dissolves in this medium.

Enzymatic Degradation

Enzymatic degradation studies of PADAS were carried out with pronase, trypsin, chymotrypsin, and papain. Results obtained with pronase, trypsin, and chymotripsin indicate that PADAS is slightly degradable by these enzymes because a negligible weight loss was observed for the discs exposed to buffers containing these enzymes.

However, a clear and steady degradation was obtained with papain. Figure 9 shows the weight loss of PADAS discs after exposure to papain. It is interesting to note that the weight loss values shown in the figure appear linearly as a function of time.

During the initial phase of degradation, the discs became white and a decrease in the thickness of the sample was clearly observed. When the disc exposure was continued beyond a 35% disc weight loss, disintegration of the discs occurred and finally, complete disc disappearance was observed, confirming that the PADAS samples were completely degradable by papain to water-soluble products.

Residual PADAS films recovered after 3 or 6 days of enzymatic exposure were analyzed for changes in molecular weight by viscometric measurements. Results showed little viscosity changes, indicating that the first phase of a enzyme-catalyzed degradation of PADAS is a surface process.

Biocompatibility

The biocompatibility of PADAS was investigated using cell culture techniques, because *in vitro* assessment of biocompatibility with permanent cell lines is a good screening method for detecting adverse effects.

The L929 mouse fibroblast attached to and proliferated on the PADAS surface. Furthermore, no differences in the doublig time between PADAS and the negative control during the exponential growth phase (24–48 h, as can be seen in Figure 10(a) were found. However, the number of cells that initially grew on PADAS surface was significantly less (Newman–Keuls test, $p < 0.01$). Figure 10(b) shows a semiconfluent culture of normal L929 fibroblast growing onto the PADAS surface after 48 h. At the maximun exposure time, 72 h, PADAS maintained the cellular growth rate of the fibroblasts, but gave a slightly cytotoxic percentage of growth inhibition with respect to the negative control (27.3%). Note also in Figure

Table V Cytotoxicity of Material Extract Determined from the Metabolic Activity Test

Material Extract	Time (h)	Concentration (%)	Meas. Abs.[a]	% Viab.[b]	% Cit.[c]
Negative control	24	100	0.3270 ± 0.00817	100.9	−0.9
Positive control	24	100	0.0410 ± 0.00173	12.7	87.3
PADAS	24	100	0.2243 ± 0.01277	69.2	30.8
PADAS	24	50	0.2790 ± 0.01518	95.0	5.0
PADAS	24	25	0.3127 ± 0.00664	103.8	−3.8
PADAS	24	10	0.3023 ± 0.00478	105.7	−5.8
Negative control	72	100	0.5378 ± 0.02821	125.8	25.8
Positive control	72	100	0.0440 ± 0.00100	9.6	90.4
PADAS	72	100	0.1080 ± 0.00181	23.7	76.3
PADAS	72	50	0.2883 ± 0.02609	70.2	29.8
PADAS	72	25	0.3637 ± 0.02258	76.5	23.5
PADAS	72	10	0.4137 ± 0.01586	87.3	12.7

[a] The absorbances indicated correspond to the average value of three samples except for the negative control in which six samples were used.
[b] Viable cells.
[c] Cytotoxicity in relation to the blank group. Percentages greater than 25% indicate a cytotoxic response.

10(a) that the phenol positive control causes a significant inhibition of cellular proliferation throughout the study, with respect to both PADAS and negative control groups.

It is important to note that the PADAS growing kinetic is similar to the negative control, and so a cytotoxic response was not evident. The main difference between the number of cells present on the surface of both materials corresponds to the initial stage when the cell adherence takes place. The results suggest that this is lower in PADAS, probably due to the physico-chemical characteristics of its surface.

A different behavior response was observed for the material extract. Thus, the results obtained in the assay of released products showed a slight cytotoxicity of PADAS on the cellular metabolic activity. This was only detected in the 100% concentration sample (30.8%) at 24 h, but this effect increased with time so that, after 72 h in contact with L929 mouse fibroblast, the cytotoxic effect at the concentration of 50% was 29.8%, and that at the concentration of 100% was 76.3%. The cytotoxic percentages of the remaining concentrations were much lower than the threshold value of 25%. (Table V). Note also that the phenol positive control induced the expected cytotoxicity.

We can deduce that the cytotoxic components of PADAS increased when we submitted the polymer to hydrolitic degradation. It is not absolutely refutable that some of these components were present in the intact material surface as fortuitous impurities (chemicals like chloroform and toluene), which could have been incorporated during synthesis and/or preparation of samples. However, it is clear that the concentration of cytotoxic components must be greater for the liquid extract than on the material surface. Furthermore, taking into account that the analysis of PADAS after 50 days at 37°C at physiological pH indicates that the polymer has been partially degraded, the toxicity attributed to the impurities would combine with the action due to the liberated oligomers.

CONCLUSIONS

The results presented in this article can be summarized as follows.

1. PADAS can be synthesized in a high yield with a two step procedure where 1,12-dodecanediol is first esterified with L-alanine and then an interfacial polycondensation is carried out.
2. The polymer can be obtained with an adequate molecular weight ($M_w \sim 24{,}100$) to ensure fiber- and film-forming properties. Moreover, good solubility characteristics have been found.
3. Calorimetric analysis shows that PADAS is stable through fusion and that transamidation-transesterification reactions do not take place during the melting process. The polymer is crystalline (ca. 40%) and presents a

complex melting peak, which may be interpreted in terms of a recrystallization process that affects different populations of crystals.
4. PADAS is hydrolytically degradable. Temperature affects the rate of degradation, which takes place preferentially through their ester bonds.
5. PADAS is also degradable by using enzymes. Papain was found to be the most effective one, in a process that occurs on the film surface.
6. Cellular proliferation is observed on the PADAS material surface when it is seeded with L929 mouse fibroblasts. A moderate cytotoxicity has been detected for the products liberated during degradation.

This research has been supported by a research grant from CICYT (MAT-97–1013). N.P. acknowledges financial support from the Comissió Interdepartamental de Recerca i Innovació Tecnològica. The authors are grateful to Dr. Antonia Araño for help in biocompatibility studies.

REFERENCES

1. D. A. Barrera, E. Zylstra, P. T. Lansbury, Jr., and R. Langer, *J. Am. Chem. Soc.,* **115,** 11010 (1993).
2. R. F. Storey and K. Shoemake, *Polym. Bull.,* **31,** 331 (1993).
3. M. Vert, M. S. Li, G. Spenlehauer, and P. Guerin, *J. Mater. Sci., J. Mater. Med.,* **3,** 432 (1992).
4. J. Kohn and R. Langer, *J. Am. Chem. Soc.,* **109,** 817 (1987).
5. W. J. Bailey and B. Gapud, *Ann. NY Acad. Sci.,* **446,** 42 (1985).
6. K. E. Gonsalves, X. Chen, and T. K. Wong, *J. Mater. Chem.,* **1,** 643 (1991).
7. N. Paredes, A. Rodriguez-Galán, and J. Puiggalí, *Polymer,* **37,** 4175 (1996).
8. R. J. Gaymans and J. L. de Haan, *Polymer,* **34,** 4360 (1993).
9. L. H. Ho and S. Huang, *Polym. Prepr. (Am. Chem. Soc. Div. Polym. Chem.),* **33**(2), 94 (1992).
10. P. W. Morgan, *Condensation Polymers: By Interfacial and Solution Methods,* Interscience Publishers, New York, 1965.
11. R. Arnon, *Methods in Enzymology,* Vol. XIX, G. E. Perlmann and L. Lorant, Eds., Academic, New York, 1970, p. 226.
12. Association Fraçaise de Normalisation (AFNOR), *Matériel médicochirurgical, biocompatibilité des implants chirurgicaux, méthodes d'extraction,* S93F, Doc. 12, PRS90 701 (1987).
13. Association Fraçaise de Normalisation (AFNOR), *Matériel médicochirurgical, biocompatibilité des implants chirurgicaux, evaluation in vitro de la cytotoxicité de materiaux et dispositifs médicaux,* S90 702 (1988).
14. B. Kaczmarczyk and D. Sek, *Polymer,* **36,** 5019 (1995).
15. I. Abu-Isa, *J. Polym. Sci. A-1,* **9,** 199 (1971).
16. G. D. Fasman, *Poly α-Amino Acids,* Marcel Dekker Inc., New York, 1967.
17. B. Wunderlich, *Macromolecular Physics,* vol. 3, Academic Press, New York, 1973, p. 161.
18. P. Peyser, *Polymer Handbook,* 3rd ed., J. Brandrup and E. H. Immergut, Eds., Wiley Interscience, New York, 1989, Chapter VI, p. 233.
19. D. W. Van Krevelen, *Properties of Polymers,* 3rd ed., Elsevier, Amsterdam, 1990, p. 133.